

# Redox Reactions of and Transformation between Cysteine–Mercury Thiolate and Cystine in Metallothioneins Adsorbed at a Thin Mercury Film Electrode

Fayi Song, Alejandro L. Briseno, and Feimeng Zhou\*

Department of Chemistry and Biochemistry, California State University,  
Los Angeles, Los Angeles, California 90032

Received November 30, 2000. In Final Form: February 22, 2001

Voltammetric studies of rabbit liver metallothioneins (MTs) adsorbed onto thin mercury films preformed onto glassy carbon electrodes were carried out in MT-free phosphate buffers in an attempt to shed light on the possible redox-modulated MT metal-transfer processes. The redox behavior of the surface-confined MTs was studied by cyclic voltammetry and differential pulse voltammetry, and the amount of MT adsorption was quantified by a flow-injection quartz crystal microbalance. Two reversible redox waves, with  $E_p$  values at  $-0.63$  and  $-0.91$  V, respectively, were observed for the first time. These values and the overall voltammetric characteristics were found to be remarkably analogous to those of cysteine adsorbates at thin mercury films. The peak at  $E_p = -0.63$  V is attributable to the reduction of the Cys–mercury thiolates formed between the adsorbed MTs and the mercury electrode, whereas that at  $E_{pc} = -0.91$  V is assigned to the reduction of Cys–Cys (cystine analogue) present in the portion of the MT adsorbate that is not in direct contact with the mercury film. The two redox waves were observed to be interchangeable through preelectrolysis at a negative potential (e.g.,  $-1.1$  V) to reduce the MT adsorbate, or at a more positive potential (e.g.,  $-0.1$  V) to oxidize the adsorbed MTs. On the basis of these voltammetric results, we proposed a simple schematic to elucidate the redox reactions of and the transformation between the cysteine–mercury thiolates and cystines that are present in the MT adsorbates under different electrochemical redox conditions. Since the electrochemical reduction of the cystine analogues in the MT adsorbates to the corresponding cysteines (a process facilitating metal complexation) and the reoxidation of the cysteine residues back to cystine analogues (a process causing metal release) are both reversible, it appears that the metal transfer between MT and a substrate might accompany the variation of the redox states of the MT–metal complexes. Our voltammetric studies of MTs thus provide supportive evidence for the mechanism of the MT metal transfer in cytoplasmic milieu proposed by Vallee and co-workers (Maret, W.; Vallee, B. L. *Proc. Natl. Acad. Sci. U.S.A.* **1998**, *95*, 3478–3482).

## 1. Introduction

Metallothionein,<sup>1–3</sup> an intracellular metalloprotein known to be involved in both regulation of essential metals and detoxification of nonessential metals, has recently generated a great deal of interest.<sup>4–18</sup> Metallothioneins

(MTs) are cysteine-rich, low-molecular-weight proteins and polypeptides of a high metal content. MTs were discovered in the late 1950s by Vallee and co-workers<sup>19,20</sup> and have been demonstrated to be transcriptionally induced by metals and a number of species.<sup>1,2</sup> Spatial structures of MTs<sup>8</sup> are shown to possess a dumbbell-like shape with two separate protein domains ( $\alpha$  and  $\beta$  domains) containing several metal–cysteine units. In the primary structure of MTs, the cysteines are present in the Cys–X–Cys, Cys–X–X–Cys, and Cys–Cys motifs (X represents an amino acid that is different from cysteine).<sup>1,2,7</sup> These motifs provide multiple cysteine–thiolate side chains capable of complexing a number of metals. All cysteines are involved in the binding of these metals.<sup>1,2,7</sup> For example, in rabbit liver MT, both Cd and Zn are tightly bound in the two domains.

The coordination of metals and the coordination number vary with the types of metals bound in the protein and the different isoforms of MTs.<sup>1,2,7</sup> Regardless of the type of coordination and the coordination number, the metal–cysteine bond is strong, with stability constants ranging between  $10^{18}$  and  $10^{22}$ .<sup>1,2,7</sup> Titration studies have shown that the relative affinity of the protein to different metals

(1) Binz, P. A.; Kagi, J. H. R. In *Metallothionein: Molecular evolution and classification*; Klaassen, C., Ed.; Birkhaeuser: Cambridge, MA, 1999.

(2) Kagi, J. H. R.; Schaffer, A. *Biochemistry* **1988**, *27*, 8509–8515.

(3) Hamer, D. H. *Annu. Rev. Biochem.* **1986**, *55*, 913–951.

(4) Jiang, L.-J.; Maret, W.; Vallee, B. L. *Proc. Natl. Acad. Sci. U.S.A.* **1997**, *95*, 3483–3488.

(5) Maret, W.; Vallee, B. L. *Proc. Natl. Acad. Sci. U.S.A.* **1998**, *95*, 3478–3482.

(6) Davis, J. J.; Hill, H. A. O.; Kurz, A.; Jacob, C.; Maret, W.; Vallee, B. L. *Phys. Chem. Commun.* **1998**, 1–11.

(7) Fischer, E. H.; Davie, E. W. *Proc. Natl. Acad. Sci. U.S.A.* **1998**, *95*, 3333–3334.

(8) Furey, W. F.; Robbins, A. H.; Winge, D. R.; Wang, B. C.; Stout, C. D. *Science* **1986**, *231*, 704–710.

(9) Brouwer, M.; Whaling, P.; Engel, D. W. *Environ. Health Perspect.* **1986**, *65*, 93–100.

(10) Brouwer, M.; Winge, D. R.; Gray, W. R. *Inorg. Biochem.* **1989**, *35*, 289–303.

(11) Fabisiak, J.; Tyurin, V. A.; Tyurin, Y. Y.; Borisenko, G. G.; Korotaeva, A.; Pitt, B. R.; Lazo, J. S.; Kagan, V. E. *Arch. Biochem. Biophys.* **1999**, *363*, 171–181.

(12) Lu, W.; Zelazowski, A. J.; Stillman, M. J. *Inorg. Chem.* **1993**, *32*, 919–926.

(13) Mason, Z. A.; Jenkins, K. D. In *Metal Detoxification in Aquatic Organisms*; Tessier, A., Turner, D. R., Eds.; John Wiley & Sons: New York, 1995; Vol. 3, pp 479–608.

(14) Olafson, R. W.; Sim, R. G. *Anal. Biochem.* **1979**, *100*, 343–351.

(15) Erk, M.; Biserka, R. *Cell. Mol. Biol.* **2000**, *46*, 2000.

(16) Fedruco, M.; Sestakova, I. *Bioelectrochem. Bioenerg.* **1996**, *40*, 223–232.

(17) Munoz, A.; Rodriguez, R. A. *Electroanalysis* **1995**, *7*, 674–680.

(18) Ruiz, C.; Rodriguez, R. A. *Anal. Chim. Acta* **1996**, *325*, 43–51.

(19) Margoshes, M.; Vallee, B. L. *J. Am. Chem. Soc.* **1957**, *79*, 4813–4814.

(20) Kagi, J. H. R.; Vallee, B. L. *J. Biol. Chem.* **1960**, *235*, 3460.

decreases in the hierarchical order  $\text{Hg}^{2+} > \text{Ag}^+ > \text{Cu}^+ > \text{Cd}^{2+} > \text{Zn}^{2+}$ .<sup>3</sup> The high affinity of MTs toward these metals has been used as evidence against the protein's role in intracellular metal transfer, since the binding constants are typically several orders of magnitude higher than that in the metal-receiving apometalloproteins. However, recent studies have shown that metals can be released from MT molecules and received by different apometalloproteins under oxidative conditions.<sup>4,5,9-11</sup> For example, Vallee and co-workers showed that the Zn-depleted sorbital dehydrogenase can serve as a Zn-receiving substrate in the presence of a variety of inorganic (e.g., ferricyanide) and biological (e.g., cytochrome *c*) redox couples.<sup>4,5</sup> In a separate study, Brouwer et al. reported that Cu-MT can act as a donor of Cu(I) for apohemocyanin.<sup>10</sup> Recent reports have suggested that a possible reason for this unconventional metal-transfer process is that metal release and incorporation by MTs are redox-modulated.<sup>4,5,9-11</sup> Such a suggestion is based on the observation that cellular glutathione (which is electroactive) appears to be involved in the metal release from MT and the subsequent transfer to a substrate.<sup>4</sup> These observations led Vallee and co-workers to propose that the metal release is facilitated by the breakage of the Cys-M thiolate bond (where M represents a metal) to form the corresponding Cys-Cys (the cystine analogue) under the oxidizing condition, whereas the metal accumulation might be realized under the reducing condition through the re-formation of the Cys-M or Cys-M-Cys entities.<sup>4,5</sup>

If the metal transfer were modulated by the redox reactions of MTs with a biological oxidant/reductant, it would be essential to measure the MT redox potentials accurately. Moreover, it is also important to pinpoint the chemical groups that are related to the electron-transfer reactions of metalloproteins.<sup>21-24</sup> The rates at which the redox reactions of MT and other metalloproteins proceed are also of biological relevance.<sup>4,5,21-24</sup> Thus far, the MT redox potentials have been measured either chemically by reacting with different oxidizing agents<sup>4,5</sup> or with voltammetric techniques.<sup>14-17,25-32</sup> Since cysteine and most of the metal ions associated with MTs (Cd, Hg, Ag, and Cu) are electroactive, electrochemical methods have been shown to be powerful means to study the redox properties of MTs.<sup>14-18,25-29,31-34</sup> Although voltammetric measurements should yield more accurate redox potential values of MTs, the voltammograms reported have shown complex behaviors, with most of the voltammetric peaks exhibiting quasi-reversible or irreversible behavior.<sup>14-18,25-29,31-34</sup> Furthermore, most electrochemical studies have almost

exclusively centered on the use of a dropping mercury electrode (DME), with only a few recent reports examining the possible heterogeneous electron-transfer reactions of MTs at solid electrodes such as carbon or gold.<sup>29</sup> The preference given to DMEs, besides the unique advantage of DMEs in precluding electrode fouling, stems from the fact that MTs can also be effectively accumulated at the Hg electrode surface for an enhanced sensitivity and for an indirect estimation of stability constants of MT for certain metals.<sup>15</sup> It is generally believed, due in part to the strongest affinity of MTs to mercury, that the labile metals (particularly Zn ions) originally present in MTs can be replaced by Hg.<sup>15-18,26,27,29,33</sup> Certain metals in solution (e.g.,  $\text{Cd}^{2+}$  added to MT solutions) have also been shown to be coordinated by the MTs accumulated at the DMEs.<sup>15-18,26,27,29,33</sup>

Thus far, the mechanism of the MT redox reactions at the mercury surface has not been fully elucidated. Rather, the peaks have been loosely assigned to the Zn-MT and Cd-MT complex oxidation peaks on the basis of the closeness of these peaks to the stripping potentials of Zn and Cd accumulated in the Hg medium.<sup>15-18,26,27,29</sup> Moreover, the use of DME, owing to the relatively short lifetime (a few seconds), limits the studies mainly to the intermediate MT forms whose labile metals might have only been partially replaced by Hg. Compounded by the complication arising from the overlapping redox peaks of the solution MTs and the MT species at the Hg surface, relating the individual voltammetric peaks to the relevant electroactive groups (e.g., cysteine, cystine, cysteine-metal complex, and/or cysteine-mercury thiolate) has been difficult or ambiguous.

We report here a simple procedure that ultimately led to the first observation of two well-resolved reversible MT redox peaks. In this procedure, thin mercury film (TMF) electrodes were exposed to a small volume of MT solution for a period of time before being transferred into a MT-free solution for the follow-up voltammetric characterization. The film-transfer experiments excluded the contribution of faradaic currents from the solution MTs. Furthermore, the extended exposure of MTs to the Hg surface ensures that the labile metals originally in the MT molecules have been largely substituted by Hg. The voltammetric behavior of the adsorbed MTs was compared to that of cysteine films formed at a TMF electrode using a similar experimental procedure. The observation of these reversible voltammetric peaks allowed us to unravel the possible electrode reactions. A simplified schematic describing the various electrode reactions of adsorbed MTs and an interesting transformation between the two reversible redox waves was put forth on the basis of the results in this work and the recent studies on the redox properties and metal-transfer processes of MTs. The amount of MT adsorbates was determined using a flow-injection quartz crystal microbalance (FI-QCM). On the basis of the schematic and the electrode reactions, we show that the metal-thiolate bonds can be readily broken under oxidation to form cystine and the cystine residues can reversibly be reduced to cysteine moieties, rendering the ability of MTs for possible metal complexation. Our results appear to support the theorem purported by Vallee and co-workers,<sup>4,5</sup> namely, that Cys-Cys (the cystine analogue) formation is favored under the oxidizing condition, whereas Cys-M or Cys-M-Cys entities present in the metal-containing MTs will be produced under the reducing condition.<sup>4,5</sup>

(21) Yeh, P.; Kuwana, T. *Chem. Lett.* **1977**, 1145-1148.

(22) Armstrong, F. A.; Hill, H. A. O.; Walton, N. J. *Acc. Chem. Res.* **1988**, *21*, 407-413.

(23) Rusling, J. F.; Nassar, A.-E. F. *J. Am. Chem. Soc.* **1993**, *115*, 11891-11897.

(24) Albery, W. J.; Eddowes, M. J.; Hill, H. A. O.; Hillman, A. R. *J. Am. Chem. Soc.* **1981**, *103*, 3904-3910.

(25) Olafson, R. *Bioelectrochem. Bioenerg.* **1988**, *19*, 111-125.

(26) Erk, M.; Biserka, R. *Anal. Chim. Acta* **1998**, *360*, 189-194.

(27) Erk, M.; Raspor, B. *J. Electroanal. Chem.* **1999**, *466*, 75-81.

(28) Munoz, A.; Rodriguez, R. A. *Electroanalysis* **1995**, *7*, 670-673.

(29) Sestakova, I.; Mihalova, D.; Vodickova, H.; Mader, P. *Electroanalysis* **1995**, *7*, 237-246.

(30) Sestakova, I.; Kopanica, M.; Havan, L.; Palecek, E. *Electroanalysis* **2000**, *12*, 100-104.

(31) Nieto, O.; Rodriguez, A. R. *Bioelectrochem. Bioenerg.* **1996**, *40*, 215-222.

(32) Mendieta, J.; Chivot, J.; Munoz, A.; Rodriguez, A. R. *Electroanalysis* **1995**, *7*, 663-669.

(33) Ruiz, C.; Mendieta, J.; Rodriguez, R. A. *Anal. Chim. Acta* **1995**, *305*, 285-294.

(34) Fedruco, M.; Sestakova, I.; Vesela, V. *Langmuir* **1996**, *12*, 2316-2322.

## 2. Experimental Section

**Chemicals.** Rabbit liver metallothionein (containing MT-I and MT-II) was obtained from Sigma (St. Louis, MO) and used without further purification. MT-I (61 amino acids) has one amino acid less than MT-II (62 amino acids), but the structure of and the number of cysteines and their relative locations in MT-I are the same as in MT-II.<sup>35</sup> Thus, for this work these two forms should be interchangeable (see also the discussion in section 3). MT solutions were prepared in a 0.1 M phosphate buffer (pH 7.5). Cysteine was obtained from Pierce Chemical Co. (Rockford, IL). Mercury and cadmium standard solutions were purchased from Aldrich Chemical Co., Inc. (Milwaukee, WI). All solutions were prepared with deionized water treated with a Millipore water purification system (Millipore Corp.). Nitric acid used for preparing the carrier and sample solutions was doubly distilled from Vycor (GFS Chemicals, Powell, OH).

**Electrodes and Cells.** Glassy carbon electrodes (3 mm diameter, Bioanalytical Systems, Inc., West Lafayette, IN) were polished down to 0.3  $\mu\text{m}$  with  $\text{Al}_2\text{O}_3$  paste and thoroughly cleaned in an ultrasonic water bath. The TMF coated onto the glassy carbon electrode is part of a one-compartment cell that also houses a platinum wire counter electrode and a Ag/AgCl reference electrode. The cell is a cylindrical polyethylene vial with an internal volume of about 1–1.5 mL. The QCM crystals used were AT-cut 9.995 MHz crystals (5 mm in diameter, ICM Technologies, Oklahoma City, OK) that were coated with polished carbon films in a keyhole shape on both sides. The area of the disk electrode was 0.212  $\text{cm}^2$ .

**Instruments.** Voltammetric measurements were carried out with a CHI 832 electrochemical analyzer (CH Instruments, Austin, TX). FI-QCM experiments were conducted using a CHI440 potentiostat/galvanostat. An acrylic QCM flow cell (ICM Technologies) with an internal volume of ca. 70  $\mu\text{L}$  was used in conjunction with a six-port rotary valve (Valco Instruments Co., Houston, TX). The QCM cell and the oscillator circuit box were housed in a Faraday cage (Elchema Inc., Potsdam, NY).

**Procedures.** Thin mercury films on glassy carbon electrodes or the polished carbon films coated onto the crystals were deposited by holding the electrode potential at  $-0.4$  V in a 5 mM  $\text{Hg}^{2+}$ /1%  $\text{HNO}_3$  solution for 5 min. The resulting mercury film has a thickness of about 100 nm, estimated from the charge consumed for the  $\text{Hg}^{2+}$  reduction. We found that this thickness is ideal since the voltammetric behaviors and the amounts of MT adsorption at the two different carbon-based mercury films are comparable. The adsorption of MT or cysteine onto the TMF electrode was accomplished by casting 10  $\mu\text{L}$  of the respective analyte solution on top of the Hg film for a predetermined period of time (e.g., 1 h). To avoid water evaporation, the electrode was kept in a sealed Styrofoam box saturated with water vapor. The TMF electrode was then rinsed with a copious amount of water and transferred into a phosphate solution for electrochemical measurements. For differential pulse voltammetric measurements, the pulse width and amplitude used were 50 ms and 50 mV, respectively. The phosphate buffer solution was thoroughly deaerated with  $\text{N}_2$  for at least 10 min prior to each measurement. Voltammograms of adsorbed cysteine were collected under a  $\text{N}_2$  atmosphere in a glovebox (Plas Labs, Lansing, MI).

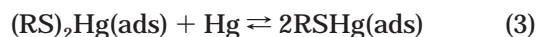
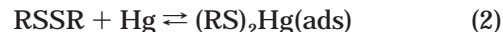
## 3. Results and Discussion

**3.1. Voltammetric Behavior of Cysteine Adsorbed onto Thin Hg Film Electrodes.** Before we discuss the voltammetric behavior of MTs adsorbed onto TMF electrodes, it is helpful to provide a short description of the voltammetric characteristics of cysteine chemisorbed onto TMF electrodes and to compare our results to findings in published papers. The reason behind this approach is related to the fact that there are 20 cysteine residues among the MT amino acids<sup>1–3</sup> and these cysteine moieties are mainly responsible for the attachment of MT molecules to the mercury surface (through the formation of the strong cysteine–mercury thiolate).<sup>1–3</sup> Both cysteine (RSH) and

cystine (RSSR) have been well-characterized voltammetrically at a variety of electrodes, such as dropping mercury and gold electrodes,<sup>36–42</sup> and the electrode reactions and voltammetric behavior have been reviewed in detail.<sup>43</sup> Briefly, at DMEs in solutions containing either of the two amino acids, two major pH-dependent reduction peaks (with prewaves) can be observed.<sup>36–42</sup> The prewaves are indicative of chemisorption of either RSH or RSSR through the following oxidation reaction:

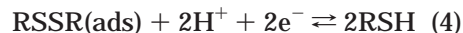


The conversion of the adsorbed RSSR to RSH is proposed to proceed in the following reactions:<sup>42</sup>



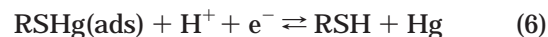
Reactions 2 and 3 suggest that the adsorption of cystine (RSSR) onto a metal surface will eventually produce a cysteine (RSH) adsorbate film. The electrochemistry of the adsorbed RSH or RSSR has been thoroughly examined by Stankovich and Bard<sup>36–38</sup> and Miller and Teva.<sup>41</sup> In a buffer solution of pH 7.4 containing cystine,<sup>36</sup> the two major reduction peaks are assigned to the following electrode reactions:

at  $-0.5$  V vs saturated calomel electrode:



at  $-0.9$  V:  $\text{RSSR(soln)} + 2\text{H}^+ + 2\text{e}^- \rightleftharpoons 2\text{RSH} \quad (5)$

In a cysteine (RSH) solution, the peak at the more positive potential ( $-0.5$  V) was also related to the reaction



which is the reverse reaction of reaction 1. The relative position for the reduction peak of the adsorbed RSSR species with respect to that of the solution species is dependent on the magnitude of the free energy of adsorption<sup>50</sup> and has also been shown to be dependent on the bulk concentration of RSSR.<sup>43</sup>

We found that cysteine in the solution droplets (10  $\mu\text{L}$ ) cast on top of the TMF electrode can be accumulated at the film surface for a certain period of time (e.g., 3 h) without an applied potential. Figure 1a shows the differential pulse voltammograms (DPVs) of cysteine adsorbed onto a TMF electrode (solid line curve for the first scan and dotted line curve for the second scan) collected in a cysteine-free phosphate buffer solution. The potential values of peak I (ca.  $-0.56$  V) and peak II (ca.  $-0.93$  V) are in excellent agreement with those reported by Stankovich and Bard.<sup>36</sup> Notice that peak II completely disappears in just one potential scan. In a separate experiment,

(36) Stankovich, M. T.; Bard, A. J. *J. Electroanal. Chem.* **1977**, *75*, 487–505.

(37) Stankovich, M. T.; Bard, A. J. *J. Electroanal. Chem.* **1977**, *85*, 173–183.

(38) Stankovich, M. T.; Bard, A. J. *J. Electroanal. Chem.* **1978**, *86*, 189.

(39) Fawcett, W. R.; Fedurco, M.; Kovacova, Z.; Borkowska, Z. *J. Electroanal. Chem.* **1994**, *368*, 275–280.

(40) Fawcett, W. R.; Fedurco, M.; Kovacova, Z.; Borkowska, Z. *J. Electroanal. Chem.* **1994**, *368*, 265–274.

(41) Miller, I. R.; Teva, J. *J. Electroanal. Chem.* **1972**, *75*.

(42) Heyrovsky, M.; Mader, P.; Vesela, V.; Fedruco, M. *J. Electroanal. Chem.* **1994**, *369*, 53–70.

(43) Ralph, T. R.; Hitchman, M. L.; Millington, J. P.; Walsh, F. C. *J. Electroanal. Chem.* **1994**, *375*, 1–15.

(35) Gui, Z.; Green, A. R.; Kasrai, M.; Bancroft, G. M.; Stillman, M. *J. Inorg. Chem.* **1996**, *35*, 6520–6529.



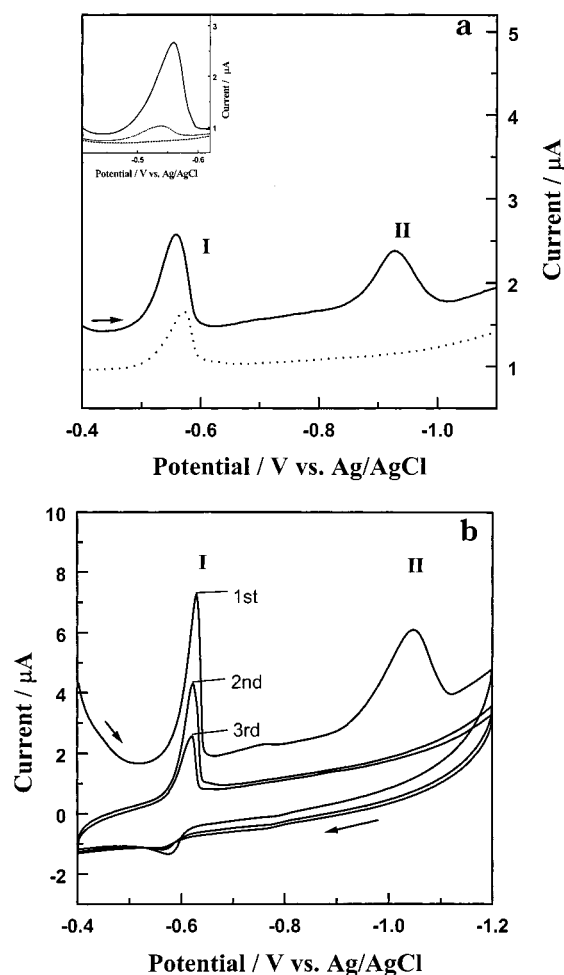


**Figure 1.** (a) Differential pulse voltammograms and (b) three consecutive cyclic voltammograms of cysteine adsorbed onto a thin mercury film electrode from a 10  $\mu$ L solution containing 10  $\mu$ M cysteine in a 0.1 M phosphate buffer (pH 7.5). The voltammograms were collected in a cysteine-free phosphate buffer. In (a), the solid line curve is the first scan and the dotted line curve represents the subsequent scan. The inset in (a) shows three consecutive DPV scans with the final potential terminated at  $-0.63$  V. Experimental conditions for DPV were pulse width = 50 ms, amplitude = 50 mV, and pulse period = 0.2 s. The scan rate for the CV experiment was 100 mV/s. Arrows in both panels indicate the scan directions.

we terminated the potential scan at  $-0.62$  V and carried out three continuous scans. The precipitous decrease of peak I (inset of Figure 1) suggests that the adsorbate can also be stripped at a potential at or more negative than peak I, though the desorption is not as effective as that observed when the potential is scanned over peak II. Previously the reductive desorption of cysteine had also been performed in a film-transfer experiment using gold as the substrate electrode.<sup>39,40</sup> Fawcett et al. observed two reduction peaks at  $-0.63$  and  $-1.4$  V, respectively, and found that about 40% of the total cysteine adsorbate is stripped at the first peak, with the rest desorbing at the latter peak.<sup>44</sup>

Since the adsorbed cysteine can be quantitatively desorbed in one potential scan over peak II, we conducted separate cyclic voltammetric (CV) experiments in an attempt to quantify the amount of cysteine originally attached to the TMF electrodes. Figure 1b shows three consecutive CV scans within the same potential range.

The combined charges under peaks I and II, averaged from voltammograms in the first potential cycles acquired at five separate TMF electrodes, led to the deduction of a surface density of  $(4.4 \pm 0.3) \times 10^{-10}$  mol/cm<sup>2</sup>. We also carried out potential step chronocoulometry to determine the charges associated with the two reduction reactions (between  $-0.4$  and  $-0.7$  V and between  $-0.7$  and  $-1.1$  V, respectively). A combined value of  $1.1 \times 10^{-9}$  mol/cm<sup>2</sup> was obtained. These values are comparable to each other considering some uncertainty may arise from the high charging current (Figure 1b). Since integration of the areas of peaks I and II in Figure 1b can exclude some of the charging current through the choice of a suitable baseline, we feel that the surface density determined from the CV experiment might be more reliable. The choice of the potential ranges in which the potential step chronocoulometry was conducted was based on the DPV shown in Figure 1a. While Figure 1a shows better-defined peaks, the ranges were widened to ensure that the initial or the final potential values were not close to or in the peak widths. Stankovich and Bard measured a cysteine surface density of  $2.3 \times 10^{-10}$  mol/cm<sup>2</sup> at a DME and suggested that it should correspond to a monolayer of cysteine.<sup>36</sup> Thus, it appears that about two monolayers of cysteines are formed at the surface of the TMF in our procedure. The contention of forming a multilayer of cysteine adsorbate at TMF electrodes is also purported by the X-ray photoelectron spectroscopic (XPS) measurements. XPS showed that cysteine films at gold substrates had a thickness of about 4.0 nm (corresponding to about eight layers, estimated using 0.49 nm as the fully extended length<sup>45,46</sup> and assuming the molecule is perpendicular to the surface). Since even multilayers of alkanethiolates can be formed at gold surfaces after a long incubation,<sup>47</sup> it is not surprising to observe two layers of cysteine films, given the fact that the zwitterionic structure tends to promote intermolecular interactions.<sup>39,40,44</sup>

If the cysteine adsorbate film is thicker than a monolayer, some of the molecules in the layer beyond the first monolayer (which is presumably anchored through the RS–mercury thiolates) could undergo dimerization to yield cystine (RSSR) upon oxidation. We found that, even if the solution was carefully degassed with N<sub>2</sub> and the entire electrochemical experiment was conducted in a glovebox, the voltammogram (not shown) did not appear to be much different than that in Figure 1. This suggests that the potential imposed to the electrode before the potential scan reaches peaks I and II might be positive enough to oxidize some cysteine molecules that are not in direct contact with the TMF surface. The electron transfer between these cysteine molecules and the electrode can be facilitated through tunneling as the thickness of one monolayer of cysteine (0.49 nm calculated using 1.54 Å as the C–C bond length and 1.81 Å as the C–S bond<sup>45</sup>) is below the tunneling barrier (i.e., 0.5–1 nm).<sup>48</sup>

Taking all of the aforementioned observations/facts into account, it appears that the RS–mercury thiolates in the first adsorbate layer undergo reductive desorption at ca.  $-0.5$  V. Unlike the desorption of short alkanethiols bearing polar tail groups in an alkaline solution (e.g., mercaptopropionic acid<sup>49</sup>), desorption of a cysteine monolayer cannot be completed in one potential scan (inset in Figure 1) and

(45) Leung, T. Y. B.; Gerstenberg, M. C.; Lavrich, D. J.; Scoles, G. *Langmuir* **2000**, *16*, 549–561.

(46) Zhang, J.; Chi, Q.; Nielsen, J. U.; Friis, E. P.; Andersen, J. E. T.; Ulstrup, J. *Langmuir* **2000**, *16*, 7229–7237.

(47) Kim, Y.-T.; McCarley, R. L.; Bard, A. J. *Langmuir* **1993**, *9*, 1941–1944.

(48) Magonov, S. N.; Whangbo, M.-H. *Surface Analysis with STM and AFM*; VCH Publishers: New York and Weinheim, 1996.

(44) Fawcett, W. R.; Fedruco, M.; Kovacova, Z.; Borkowska, Z. *Langmuir* **1994**, *10*, 912–919.

does not result in the desorption of a large amount of cysteine molecules situated beyond the first monolayer. The incomplete stripping is understandable, since it has been suggested that the zwitterionic structure of cysteine can induce intermolecular interactions, such as electrostatic attraction<sup>43</sup> or hydrogen bonding.<sup>46</sup> Moreover, the low aqueous solubility of cysteine (RSSR)<sup>43</sup> favors the hydrophobic interaction between the amino acid and the electrode.

Peak II at  $-0.93$  V, therefore, is assigned to the reduction of cystines (RSSR) present in the second layer of the cysteine film. Such a conclusion is partially drawn from the suggestion that RSSR in the vicinity of a TMF electrode (but not in direct contact with the surface) undergoes reduction to its thiol counterpart at this potential (see reaction 6).<sup>36</sup> Considering that a similar observation has been made at a cysteine-modified gold electrode,<sup>39,40,44</sup> our conclusion appears to be reasonable.

**3.2. Voltammetric Behavior of MTs Adsorbed onto Thin Hg Film Electrodes.** Similar to cysteine, MTs can also be attached onto a TMF electrode using the same procedure and the TMF electrode covered with MT molecules can be subsequently transferred to a MT-free solution for the electrochemical characterization. Shown in Figure 2a are two consecutive DPV scans (solid line curve for the first scan and dotted line curve for the second) in the negative-going direction. Two peaks, labeled 1 and 2, were observed at  $-0.63$  and  $-0.91$  V, respectively. The two DPVs are essentially congruent, suggesting that the MT film is very robust and will not be reductively desorbed. In fact, potential cycles can be implemented continuously for as long as 20–30 min without any appreciable signal degradation. Figure 2b is a representative cyclic voltammogram of adsorbed MT after five potential cycles. As can be seen, two well-defined reversible redox waves can be observed in the potential range of Figure 2a. The reduction potentials of the MT adsorbates are remarkably analogous to that of the cysteine film. Both peaks have a potential splitting ( $\Delta E_p$ ) of 30 mV. To further substantiate the adsorbate nature of the MT molecules, we performed an analysis of the dependence of peak currents ( $i_{pc}$  or  $i_{pa}$ ) on the scan rate,  $\nu$ , ranging from 50 to 500 mV/s. The normalized  $i_{pc}$  values of both peaks 1 and 2 were found to increase linearly with the normalized scan rate:  $i_{\text{normalized}} = 1.17\nu_{\text{normalized}} - 0.24$  ( $R^2 = 0.999$ ) for peak 1 and  $i_{\text{normalized}} = 0.85\nu_{\text{normalized}} + 0.34$  ( $R^2 = 0.994$ ). As can be seen in Table 1, the  $i_{pc}/i_{pa}$  ratios for peaks 1 and 2 are 1.2 and 0.8, respectively. Considering that various factors, such as inhomogeneity of the film, the finite charge transport, and structural and resistive changes in the film,<sup>50</sup> can all lead to peak asymmetry, the small peak splitting and the nearly unit peak current ratios suggest that the voltammetric peaks are reversible and should be originated from surface-confined species. Previous voltammetric studies of MTs at DMEs in MT-containing solutions have shown multiple redox peaks of adsorbed MTs and MTs in the solution near the electrode surface. For example, in the first work on the MT electrochemistry reported by Olafson,<sup>25</sup> the four or more overlapping peaks of MTs isolated from the scrab *Scylla serrata* made the elucidation of the electrode processes difficult. MT voltammograms consisting of 3–4 quasi-reversible waves<sup>16</sup> or peaks with shoulder waves<sup>17,18,27</sup> have also been shown in several recent studies. The multiple redox processes associated with the surface-bound and the solution species, the

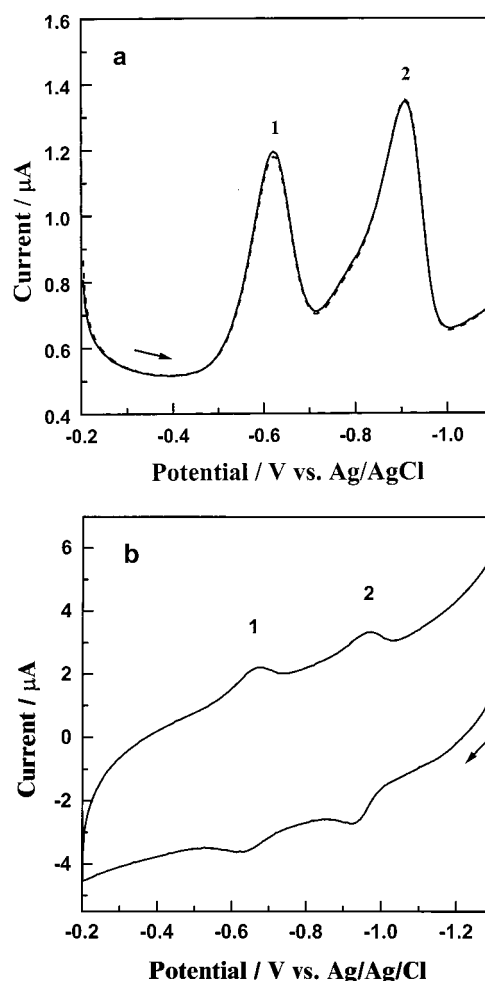


**Figure 2.** Differential pulse voltammograms (a) and a cyclic voltammogram (b) of rabbit liver MTs adsorbed onto a thin mercury film electrode from a  $10\ \mu\text{L}$  solution containing  $22\ \mu\text{M}$  MT in a  $0.1\ \text{M}$  phosphate buffer (pH 7.5). In (a), two consecutive scans were carried out and the experimental parameters are the same as those in Figure 1a. In (b), the scan rate used was  $0.2\ \text{V/s}$ . In both panels, arrows indicate the initial scan direction.

possible involvement of metals, and the replacement of the metals inherent in MTs by Hg greatly complicate the interpretation of the MT voltammetric responses. The clarity and the reversibility of these peaks depicted in Figure 2 are in contrast with those of most of the published voltammograms on various MTs, due in part to the following two improvements. First, the film transfer excluded the complication introduced by the redox reactions of solution MTs. Second, the extended exposure of the solution droplet containing MTs to the mercury surface probably facilitated the significant replacement of the pristine MT metals (e.g.,  $\text{Cd}^{2+}$  and  $\text{Zn}^{2+}$ ) by mercury.<sup>3</sup> Finally, the ruggedness of the MT films enabled us to conduct a series of voltammetric experiments described in the following, providing an opportunity to investigate the mechanism of the redox processes of adsorbed MTs.

Since the potentials of peaks 1 and 2 of Figure 2 are very close to those of peaks I and II of Figure 1, it is reasonable to think that the same electroactive groups should be responsible for the observed electrode processes. If the extrapolation is valid, the electrode reaction corresponding to peak 1 in Figure 2a should arise from the reduction of the thiolates formed between the cysteine residues on MTs and mercury. Obviously the ruggedness of the MT film defies the mechanism of reductive desorption of MTs. We think that this can be explained on

(49) Porter, M. D.; Weisshaar, D. E.; Lamp, B. D. *J. Am. Chem. Soc.* **1992**, *114*, 5860–5862.

(50) Bard, A. J.; Faulkner, L. R. *Electrochemical Methods. Fundamentals and Applications*; John Wiley & Sons: New York, 2001.

**Table 1. Representative Peak Potentials, Currents, Potential Splittings, and Areas for the Two Reduction Waves of Metallothioneins**

peak	$E_{pc}$ (V)	$E_{pa}$ (V)	$\Delta E_p$ (V)	$i_{pc}$ ( $\mu$ A)	$i_{pa}$ ( $\mu$ A)	$A_{pc}$ ( $\times 10^8$ AV) <sup>a</sup>
peak 1 (Figure 2b)	-0.66	-0.63	0.03	$0.56 \pm 0.04$	$0.53 \pm 0.06$	
peak 2 (Figure 2b)	-0.96	-0.93	0.03	$0.51 \pm 0.04$	$0.65 \pm 0.04$	
peak 1 (Figure 4a)	-0.63			$0.54 \pm 0.04$		$5.5 \pm 0.6$
peak 2 (Figure 4a)	-0.91			$0.20 \pm 0.03$		$1.6 \pm 0.3$
peaks 1 + 2 (Figure 4a) <sup>b</sup>						$7.1 \pm 0.7$
peak 2 (Figure 4d) <sup>c</sup>	-0.91					$6.4 \pm 0.3$

<sup>a</sup> Integrated area of each peak. <sup>b</sup> Summation of the two peak areas before the transformation. <sup>c</sup> Area of peak 2 after the complete transformation.

the basis of electrostatic attraction. At neutral pH, the positively charged amino acids (7–8 lysines per MT-I or MT-II) outnumber the negatively charged amino acids (2–3 aspartates per MT-I or MT-II).<sup>51</sup> Consequently, the overall MT molecules are positively charged. The potential around or beyond peak 1 has been shown by electrocapillary measurements to be more negative than the point of zero charge (PZC) at a mercury surface.<sup>34,42</sup> Thus, the MT molecules, upon the breakage of the cysteine–mercury thiolate bond(s), will still be attached to the Hg surface via electrostatic attraction.

If we likened the redox behavior of adsorbed MTs to that of cysteine adsorbates, peak 2 in Figure 2a should be ascribed to the reduction of cystine (RSSR) analogues that are not in direct contact with the mercury to the cysteines. This proposition would be valid only if the following premises were held: (1) Not all of the 20 cysteines on each MT molecule had formed cysteine–mercury thiolates. (2) Upon the initiation of the potential scan at -0.4 V and en route to peaks 1 and 2, some of the Cys–M or Cys–M–Cys complexes in the MT molecules (where M represents a divalent metal such as Hg, Zn, or Cd) had been converted to the cystine analogue (RSSR). (3) There must exist MT adsorbates with different surface structures. Evidence and/or arguments supporting points 1 and 2 are given in this section, whereas an interesting observation closely related to point 3 is discussed in section 3.3.

To address point 1, it is imperative to know the amount of MT adsorbed on the TMF electrode and the average number of cysteines per MT molecule involved in the RS–Hg bond formation and breaking. Recently, Hill, Vallee, and co-workers reported the first scanning tunneling microscopic (STM) imaging of MTs chemisorbed onto a gold surface and showed that the typical flattened MT molecule has an oval or rectangular surface feature with a width of about 1.5 nm and a length of about 3 nm.<sup>6</sup> Thus, the surface area occupied by a MT molecule will be about 4.5 nm<sup>2</sup> (assuming that the MT molecule resembles a rectangle). In other words, the highest possible number of MT molecules per square centimeter would be 1 cm<sup>2</sup> / (4.5  $\times$  10<sup>-14</sup> cm<sup>2</sup>/molecule) = 2.22  $\times$  10<sup>13</sup> molecules. This would correspond to a surface density of 3.7  $\times$  10<sup>-11</sup> mol/cm<sup>2</sup> when all the MT molecules are closely packed onto the surface. We compared this maximum surface density to the value deduced from a FI-QCM measurement of the MT adsorption. A typical response at a crystal covered with a mercury film to the injected MT solution is shown as the solid line curve in Figure 3. The control experiment (dotted line curve) indicates that the injection of a MT-free phosphate buffer into the carrier would not cause any discernible mass change. The instantaneous mass increase immediately after the MT solution enters into the cell suggests that the MT adsorption is a rapid process.

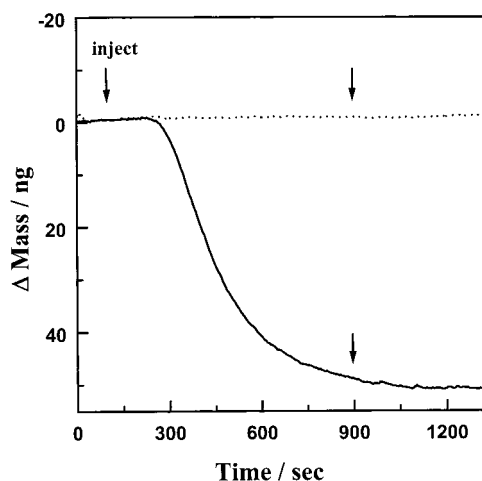


**Figure 3.** Time-resolved QCM responses at QCM crystals coated with thin mercury films to the injections of 100  $\mu$ L of phosphate buffer solution containing 22  $\mu$ M MT (solid line curve) and 100  $\mu$ L of MT-free phosphate solution (dotted line curve). The arrows indicate the time at which the injection was made and the time when the injected samples were completely replaced by the carrier solution. The flow rate employed was 10  $\mu$ L/min.

Although it is widely accepted that some of the pristine metals in the MT molecules (e.g., Zn<sup>2+</sup> and Cd<sup>2+</sup>) can be replaced by mercury<sup>15–18,26,27,29</sup> (see also the hierarchical order described in the Introduction), the mass increase caused by the loss of these metals would not be significant enough to change the overall QCM response. The average MT molecular weight calculated on the basis of the amino acid content is about 6800, whereas the average molar mass associated with all the Cd<sup>2+</sup> and Zn<sup>2+</sup> in a MT molecule is about 350.<sup>51</sup> Thus, the mass of the metals is only a small fraction of the total mass of the MT molecule. Consequently, we can deduce the amount of MT adsorbate from the mass change with a reasonable accuracy. Using the Sauerbrey equation,<sup>52,53</sup> the mass change averaged from three separate FI-QCM measurements (51.6 ng) yielded a surface density of 3.5  $\times$  10<sup>-11</sup> mol/cm<sup>2</sup>. Interestingly, this value corresponds to 95% of a monolayer, if compared to the value calculated on the basis of the size of MT determined by STM.<sup>6</sup> This suggests that, unlike the cysteine adsorption, formation of multilayers of MTs does not appear to occur at the metal electrode surface. This is consistent with the submonolayer surface coverage of the MT adsorbates at the gold substrate.<sup>6</sup> The monolayer or submonolayer coverage is expected considering that the amino acids within the folded portion of a protein molecule are not very accessible spatially. As a result, the intermolecular interaction among the individual amino acids is not facilitated. Moreover, the electrostatic repul-

(51) Stillman, M. J.; Shaw, C. F. I.; Suzuki, K. T. *Metallothioneins. Synthesis, structure and properties of metallothioneins, phytochelatins and metal–thiolate complexes*; VCH Publishers: New York, 1992.

(52) Ward, M. D.; Buttry, D. A. *Science* **1990**, *249*, 1000–1007.

(53) Buttry, D. A. In *Electroanalytical Chemistry*; Bard, A. J., Ed.; Marcel Dekker: New York, 1991; Vol. 17.



sion (all of the MT molecules possess some positive charges, vide infra) prevents the MT molecules from being packed very tightly or interlocked together.

The integration of the area under peak 1 ( $3.9 \pm 0.5 \mu\text{C}/\text{cm}^2$ ) should provide the charges associated with the reduction of the RS–mercury thiolates. We estimated the amount of RS–Hg per unit area that has undergone reduction to be  $4.1 \times 10^{-11} \text{ mol}/\text{cm}^2$ , assuming that one electron is involved under peak 1 (i.e.,  $n = 1$ ). This value is slightly larger (1.17 times) than that measured from the FI-QCM experiment ( $3.5 \times 10^{-11} \text{ mol}/\text{cm}^2$ ). Thus, the comparison of the voltammetric and the FI-QCM results strongly suggests that not all of 20 cysteine residues in a MT molecule (i.e.,  $n$  would be 20) have formed the Cys–mercury thiolate bonds and participated in the first reduction reaction. We caution that the MT adsorbate most likely did not form a rigid film and consequently the mass change measured by the FI-QCM may not all be attributable to the attachment of the MT molecules. Previous studies<sup>54–56</sup> have shown that the QCM response to protein layers may not strictly follow the Sauerbrey equation due to the different factors such as density, viscosity, and solvation. As a consequence, the actual mass change could be overestimated by as many as 4 times.<sup>56</sup> Nevertheless, the overestimation due to protein hydration and the viscosity factor would only increase the  $n$  value to a maximum of 4–5. Thus, the uncertainty will not be significant enough to alter the value by more than an order of magnitude (i.e., from  $n = 1$  to  $n = 20$ ).

The cysteine groups that did not form the cysteine–mercury thiolates could bind to metal ions in the form of Cys–M and/or Cys–M–Cys complexes (where M can be Hg, Cd, or Zn).<sup>1–3,7,8</sup> While the complexation constants for forming the Cys–M bonds are high,<sup>1–3</sup> recent work by Vallee and co-workers has shown that a variety of relatively mild oxidizing reagents can lead to the breakage of the Cys–M bond and the formation of the Cys–Cys disulfide. In the work by Vallee and co-workers,<sup>4,5</sup> homogeneous chemical redox reactions between MTs and oxidizing reagents were studied and the metal release from MTs to apometalloenzymes was quantified. These researchers found the lower limit for oxidizing MTs to be at  $-0.37 \text{ V}$  vs normal hydrogen potential (or  $-0.56 \text{ V}$  vs Ag/AgCl).<sup>4,5</sup>

If the cysteine moieties in a MT molecule can be oxidized at a potential that is more positive than  $-0.56 \text{ V}$ , the initiation of a potential scan at  $-0.1$  or  $-0.2 \text{ V}$  would most certainly trigger the MT oxidation. As a consequence, certain Cys–M or Cys–M–Cys bonds could be converted to the Cys–Cys dimers (or the cystine analogue), accompanied by a simultaneous metal release. The reversibility of peak 2, which is presumed to relate to the redox reaction of the adsorbed cysteine/cystine couple, also suggests that such a conversion could be facile. An interesting observation is that  $i_{\text{pc1}}$  and  $i_{\text{pc2}}$  are comparable (Table 1). Potential step chronocoulometry also shows comparable charges under peaks 1 and 2 ( $6.1$  and  $4.1 \mu\text{C}/\text{cm}^2$ , respectively). These results imply that, on an average, the two types of reactants undergoing the two separate electrode reactions are of similar abundance. Thus, both voltammetric and FI-QCM experiments indicate that there are two types of electroactive groups of similar surface concentration that can both undergo electron transfer with

the electrode. Unfortunately, the limited mechanistic understanding of the MT adsorption process and the incompatibility of the mercury film to many surface characterization techniques that can be used to address this issue (e.g., surface plasmon resonance,<sup>57,58</sup> ellipsometry,<sup>50</sup> and scanning probe microscopy<sup>48</sup>) introduce difficulty in probing the MT surface orientation, in pinpointing the locations of the cysteine groups, and in determining the exact numbers of Cys–mercury thiolates and Cys–Cys dimers involved in the electrode reactions.

Identifying metals released from MTs, studying the correlation between the applied potential and the metal release, and investigating the adsorption behavior of MTs at TMF electrodes are beyond the scope of this work, but will be addressed in our future work. Here we need to mention that other researchers have observed that, under electrochemical oxidation(s), metals such as Cd can be released and quantified.<sup>26,27</sup> It is also worthwhile to point out that we did not observe the Cd or Zn stripping peaks superimposed onto peaks 1 and 2, suggesting that the prolonged adsorptive contact of MTs at TMF electrodes may have caused irreversible metal substitutions. Due to the absence of the labile  $\text{Zn}^{2+}$  and  $\text{Cd}^{2+}$ , anodic stripping peaks of free  $\text{Zn}^{2+}$  and  $\text{Cd}^{2+}$  reported by other researchers were not observed. The stripping peaks of Zn and Cd accumulated from  $\text{Zn}^{2+}$  and  $\text{Cd}^{2+}$  standard solutions were found to be at  $-1.15$  and  $-0.73 \text{ V}$  (data not shown), respectively, and are therefore quite different from peaks 1 and 2 of Figure 2. Furthermore, the formation of the Cys–Cys dimer under oxidative conditions purported by Vallee and co-workers<sup>4,5</sup> has an important implication in the interpretation of our data. On the basis of the current state of knowledge about the MT redox property, we think that a situation analogous to the electron transfer between a mercury electrode and several layers of cysteines (e.g., the two layers of cysteines deduced from Figure 1) might also be encountered here. Therefore, it is conceivable that the oxidized cysteines (the cystine analogue) will become reduced at a potential around  $-0.9 \text{ V}$ . Given the remarkable similarity between the redox behavior of MT adsorbates and that of cysteine films and the consistency of our data interpretation with the information about the MT redox behavior and the MT surface coverage and structure, we feel that our proposed mechanism is plausible. As will be seen in the following section, this mechanism can also explain an interesting phenomenon concerning the transformation between the Cys–mercury thiolate and the cystine entity associated with the adsorbed MTs.

**3.3. Electrochemical Transformation between the Cys–Mercury Thiolate and the Cystine Analogue Associated with the Adsorbed MTs.** In the electrochemical characterization of the adsorbed MTs, we discovered that peaks 1 and 2 could be transformed into one another under certain experimental conditions. If the electrode potential is held at  $-1.2 \text{ V}$  for a certain period of time (e.g., 60 s), peak 2 will increase at the expense of peak 1 during the DPV scan in the cathodic direction. The enhancement of peak 2 and the diminishing of peak 1 depend on the preelectrolysis time at  $-1.2 \text{ V}$ . Figure 4 shows the gradual transformation of peak 1 to peak 2 via varying the preelectrolysis time. Clearly, curve d shows that an extensive preelectrolysis can quantitatively convert peak 1 to peak 2. The areas of both peaks before and after this transformation are summarized in Table 1. The reverse transformation (from peak 2 to peak 1) can

(54) Cavic, B. A.; Hayward, G. L.; Thompson, M. *Analyst* **1999**, *124*, 1405.

(55) Martin, S. J.; Spates, J. J.; Wessendorf, K. O.; Schneider, T. W.; Huber, R. J. *Anal. Chem.* **1997**, *69*, 2050–2054.

(56) Rickert, J.; Brecht, A.; Gopel, W. *Anal. Chem.* **1997**, *69*, 1441–1448.

(57) Tao, N. J.; Boussaad, S.; Huang, W. L.; Arechabaleta, R. A.; D'Agnes, J. *Rev. Sci. Instrum.* **1999**, *70*, 4656–4660.

(58) Boussaad, S.; Pean, J.; Tao, N. J. *Anal. Chem.* **2000**, *72*, 222–226.

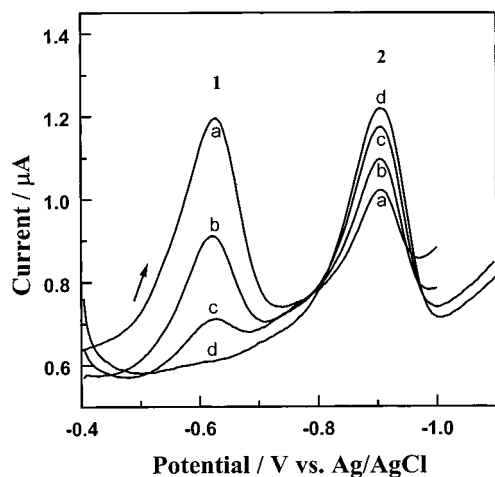


**Figure 4.** Differential pulse voltammograms of MTs adsorbed onto a mercury film electrode collected after preelectrolysis of the surface-confined MT adsorbates at  $-1.1$  V for various amounts of time. Curves a, b, c, and d were collected 0, 60, 180, and 300 s after the preelectrolysis step, respectively. The arrow indicates the scan direction, and the experimental parameters are the same as those employed for collecting the voltammograms in Figure 2a.

be accomplished by preelectrolysis at a potential more positive than that of peak 1. By holding the potential at  $-0.1$  V for a certain period of time (e.g., 1 min), the intensity of peak 2 was lessened while the height of peak 1 became greater.

To summarize the interpretation of the electrode reactions of adsorbed MTs and the above transformation process, we put forth a simplified schematic (Figure 5). Specifically, a MT molecule can be adsorbed onto TMF electrodes through the formation of Cys–mercury thiolates. The MT surface structure could be different from the native conformation because the cysteine–mercury thiolate formation might have reoriented the MT primary structure. Regardless of the surface structure, it appears that there exists a certain amount of Cys–M or Cys–M–Cys complexes that have not been disrupted by the MT adsorption process. Upon a potential scan, prior to reaching peak 1 ( $E > E_{pc1}$  in Figure 5), the electrode potential is more positive than the cysteine oxidation potential. As a consequence, a certain number of the Cys–M and/or Cys–M–Cys complexes can be dissociated

to form the cystine counterparts. This process is probably also coupled with a simultaneous metal release. When the potential is scanned over peak 1, the reduction of the Cys–mercury thiolates does not detach MTs from the electrode. At this point, the electrode potential at or beyond peak I ( $E < E_{pc1}$ ) has become more negative than the PZC.<sup>34,42</sup> Consequently, the positive charges on the MT molecules (residing at the lysine residues, shown as the empty circles in Figure 5) will confine the MT molecules to the negatively charged electrode surface. After the potential is swept over peak 2 ( $E < E_{pc2}$  in Figure 5), the cystine entities created earlier in the scan can be subsequently reduced, much in the same way as for the reduction of solution RSSR (reaction 5 shown in section 3.1) or the RSSR present in the stacked cysteine multilayers (vide supra).

Conversely, during the scan reversal in the anodic direction, two cysteines can be combined to form the cystine analogue ( $E > E_{pa2}$ ). This process is then followed by the re-formation of the Cys–mercury thiolate bonds ( $E > E_{pa1}$ ). The Cys–mercury thiolate formation might induce some structural changes, since some of the cysteine residues will get back onto the TMF electrode surface at this point.

Finally, a DPV of the MT adsorbates that had been completely transformed into the completely reduced form (e.g., all to peak II) in the anodic scan is shown as the solid line curve in Figure 6. The completely reduced MT adsorbates should not contain any Cys–mercury thiolates and cystines. We hypothesize that extensive preelectrolysis of the MT adsorbates had somehow rearranged/reoriented the MT molecules at the surface so that the reattachment of the MT molecules to the mercury surface through the Cys–mercury thiolate bonds could not be rapidly accommodated. In other words, although the cysteine residues have a strong affinity to the mercury surface once the mercury surface is oxidized (a prerequisite for the Cys–mercury thiolate formation as suggested by reaction 1), the spatial obstruction to the approach of the cysteine groups to the TMF surface by the newly arranged MT molecules impedes the reattachment process. The suggestion of a possible structural change is not totally unsubstantiated. There are at least two separate reports that provide supportive evidence about a possible reorientation. First, in the report by Stillman and co-workers,<sup>59</sup> the MT structure, upon exposure to a high dosage of mercury, was revealed by circular dichroism to possess a

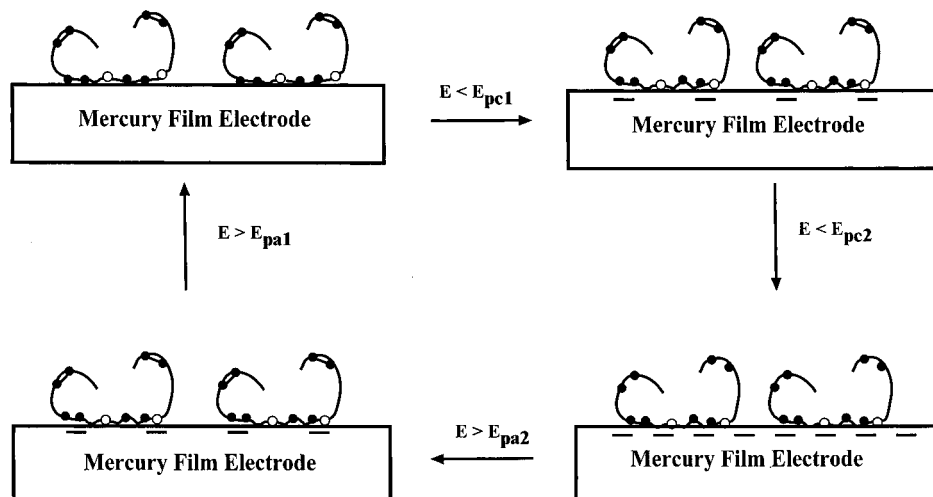


**Figure 5.** Simplified schematic representation of the MT adsorbates undergoing redox reactions at different potentials. The filled circles represent the cysteine or cystine residues, and the empty circles represent the positive charges on the lysine residues. The linkage of two cysteines to form one cystine analogue is represented by a solid line.



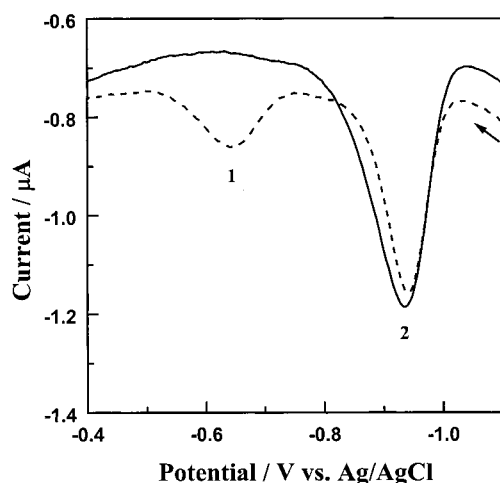


**Figure 6.** Differential pulse voltammograms of the adsorbed MTs in the anodic scan immediately after a preelectrolysis of the MT adsorbates at  $-1.1$  V for 300 s, and at the same MT-modified thin mercury film electrode after preelectrolysis at  $-1.1$  V for 300 s, followed by a reoxidation at  $-0.1$  V for 60 s.

3-dimensional framework based on a single domain that is rather different from the native conformation of MTs. Second, in the electrochemical studies of insulin (which contains three Cys-Cys disulfide bonds) at DMEs, Stankovich and Bard suggested that reduced sulfurs or sulfhydryls in the adsorbed insulin could change their orientation with respect to one another.<sup>37</sup> We should add that these researchers also noted that reoxidation of all the reduced sulfhydryls in the insulin adsorbates could be realized at short times, but the conversion was not complete because of the orientation changes.<sup>37</sup> Therefore, it appears that, at the mercury surface, certain cysteine-containing proteins can undergo orientation changes to either facilitate (by moving two cysteines closer) or hamper (by moving two cysteines further away) the disulfide bond formation. Referring to Figure 5, upon extensive preelectrolysis at  $-1.1$  V, the detachment of the cysteine residues from the mercury surface would result in subsequent dimerization reactions between adjacent cysteines that were originally involved in the Cys-mercury thiolate formation. From the viewpoint of spatial arrangement, the dimerization is highly possible, because the cysteines are present in the Cys-Cys, Cys-X-Cys, and Cys-X-X-Cys motifs. In other words, the filled circles in the MT structure that are closer to the mercury surface (Figure 5) can also form disulfide linkages upon extensive electrolysis. The dimerization to the cystine analogue (RSSR) can decrease the rate of the re-formation of the Cys-mercury thiolates (or oxidative adsorption as shown by reaction 1), since Whitesides and co-workers noted that adsorption of thiols onto metal surfaces is strongly favored over that of disulfides.<sup>60,61</sup>

To verify that the reattachment of the MT molecules through the formation of the Cys-mercury thiolates is indeed modulated by the potential and the time duration for the preelectrolysis, we oxidized the completely transformed MT adsorbate at  $-0.1$  V for 60 s. The dotted line curve in Figure 6 shows the voltammogram acquired during a DPV scan in the anodic direction right after the oxidation step. As can be seen, peak 2 has decreased

slightly and peak 1 has become discernible. It is thus clear that the transformation process is intricately related to the accessibility of the electroactive groups to the electrode surface, which, in turn, is governed by the orientations adopted by the MT molecules. Given the complexity associated with the 3-dimensional structures of MTs, the electrostatic and covalent interactions between the protein and the electrode surface, and the aforementioned lack of surface structural information available at the mercury surface, we feel that the model depicted in Figure 5 can reasonably explain both the redox reactions and the transformation between the two cysteine-containing moieties in the MT adsorbates.

#### 4. Conclusions

A simple procedure for accumulating MTs onto TMF electrodes for the subsequent electrochemical characterization in a MT-free buffer solution has been developed. The extended time for exposing the adsorbed MTs to the mercury surface and the film-transfer step eliminated several overlapping peaks and prewaves shown in the literature. Moreover, the use of a TMF enabled us to utilize a FI-QCM to quantify the amount of MT adsorption (a technique incompatible with mercury drops). Two well-resolved reversible voltammetric waves have been observed. The clarity of the voltammetric waves and the robustness of the MT adsorbate film allowed a thorough voltammetric characterization with an excellent repeatability. The voltammogram has a marked resemblance to that of the cysteine film at a TMF electrode in terms of the peak potentials. Through the comparison of the redox behavior of the adsorbed MTs to that of the adsorbed cysteine and taking into account results published by other laboratories, we assigned the wave at  $-0.63$  V to the reduction of the cysteine-mercury thiolate and the wave at  $-0.91$  V to the reduction of the Cys-Cys dimer present in the MT adsorbates upon electrochemical oxidation. This assignment is in line with the well-studied cysteine/cystine electrochemistry and the recently reported MT oxidation reactions and metal transfer induced by various chemical redox species. This work also revealed, for the first time, that the two redox waves are interchangeable upon preelectrolysis at a reducing potential or an oxidizing potential and the transformation is influenced by the time duration in which the preelectrolysis is conducted. Our voltammetric characterization of the MT adsorbates and the FI-QCM quantification of the MT adsorption help elucidate the interplay between the redox reactions of the electroactive groups and the overall MT redox property. The development of the procedure and the insight gained about this system may offer a potential opportunity to correlate the redox potential(s) of MTs to the metal-transfer processes. Probing the possible redox-modulated metal-transfer processes is very important for the explication of the biological function of MTs in the cellular environment. The exploration of different MT immobilization schemes that will allow one to characterize the surface structures of the adsorbed MT molecules under different electrochemical conditions is in progress.

**Acknowledgment.** Partial support for this work by a NSF-CRUI grant (DBI-9978806), a NIH-SCORE grant (GM08101), and the Center for Environmental Analysis at CSULA is gratefully acknowledged. We thank Prof. A. Z. Mason and Mr. A. J. Baca for their helpful discussions. We are also grateful to Darell Brehm (ICM Co., Inc.) for the generous donation of the polished carbon-coated quartz crystals.

(59) Stillman, M. J.; Law, A. Y. C.; Cai, W.; Zelazowski, A. J. *Exp. Suppl.* **1987**, 52, 203–211.

(60) Bain, C. D.; Evall, J.; Whitesides, G. M. *J. Am. Chem. Soc.* **1989**, 111, 7155–7164.

(61) Bain, C. D.; Whitesides, G. M. *J. Am. Chem. Soc.* **1989**, 111, 7164–7175.